8. Alpagut, B., Andrews, P. & Martin, L. New hominoid specimens from the Middle Miocene site at Pasalar, Turkey. *J. Hum. Evol.* **19,** 397–422 (1990).
9. Barry, J. C. *et al.* Faunal and environmental change in the Late Miocene Siwaliks of northern Pakistan. *Paleobiology Memoirs* **3**(28), 1–71 (2002).
10. Morgan, M. E., Kingston, J. D. & Marino, B. D. Carbon isotopic evidence for the emergence of C4 plants in the Neogene from Pakistan and Kenya. *Nature* **367,** 162–165 (1994).
11. Cerling, T. E. *et al.* Global vegetation change through the Miocene/Pliocene boundary. *Nature* **389,** 153–158 (1997).
12. Pajunen, H. *Proc. Symp. Int. Peat Soc., Jamaica, 25 February–1 March 1985* (ed. Heikurainen, L.) 186–197 (Int. Peat Soc., Helsinki, 1985).
13. Badgley, C., Guoqin, Q., Wanyong, C. & Defen, H. Paleoecology of a Miocene, tropical, upland fauna: Lufeng, China. *Nat. Geogr. Res.* **4,** 178–195 (1988).
14. Hooijer, D. A. Prehistoric teeth of man and of the orang-utan from central Sumatra, with notes on the fossil orang-utan from Java and Southern China. *Zool. Med.* **29,** 175–301 (1948).
15. Kelley, J. & Plavcan, J. M. A simulation test of hominoid species number at Lufeng, China: implications for the use of the coefficient of variation in paleotaxonomy. *J. Hum. Evol.* **35,** 577–596 (1998).
16. Kelley, J., Anwar, M., McCollum, M. A. & Ward, S. C. The anterior dentition of *Sivapithecus parvada*, with comments on the phylogenetic significance of incisor heteromorphy in Hominoidea. *J. Hum. Evol.* **28,** 503–517 (1995).
17. Wu, R. & Oxnard, C. E. Ramapithecines from China: evidence from tooth dimensions. *Nature* **306,** 258–260 (1983).
18. Swarts, J. D. in *Orangutan Biology* (ed. Schwartz, J. H.) 263–270 (Oxford University Press, London, 1988).
19. Martin, L. Significance of enamel thickness in hominid evolution. *Nature* **314,** 260–263 (1985).
20. Martin, L. *The Relationships of the Later Miocene Hominoidea*. Thesis, Univ. London (1983).
21. Schwartz, J. H. in *Function, Phylogeny, and Fossils: Miocene Hominoid Evolution and Adaptations* (eds Begun, D. R., Ward, C. V. & Rose, M. D.) 363–388 (Plenum, New York, 1997).
22. Schwartz, J. H. *Lufengpithecus* and its potential relationship to an orang-utan clade. *J. Hum. Evol.* **19,** 591–605 (1990).
23. Harrison, T. & Rook, L. in *Function, Phylogeny, and Fossils: Miocene Hominoid Evolution and Adaptations* (eds Begun, D. R., Ward, C. V. & Rose, M. D.) 327–362 (Plenum, New York, 1997).
24. Remus, D., Webster, M. & Krawkan, K. Rift architecture and sedimentology of the Phetchabun intermontane basin, central Thailand. *J. Southeast Asian Earth Sci.* **8,** 421–432 (1993).
25. Johnson, N. M. & McGee, V. E. Magnetic polarity stratigraphy: stochastic properties of data, sampling problems, and the evolution of interpretations. *J. Geophys. Res.* **88,** 1213–1221 (1983).

Acknowledgements We thank P. Andrews, L. de Bonis, J. Kappelman, J. Kelley and D. Pilbeam for comments, help, discussion and providing comparative materials; J. H. Schwartz and J. Kappelman for improving our manuscript; E. Boller, J. Baruchel and the ID 19 beamline staff of the European Synchrotron Radiation Facility (Grenoble, France) for their help in obtaining microtomographic images; A. Sritulakarn and N. Wongchai for providing facilities in Chiang Muan coal mine; B. Marandat for preparing fossils and making casts; H. Tong for translating Chinese documents; J. Barry, P. Tassy, G. Métais and S. Ducrocq for identifying associated large mammals. This work was supported by the Wenner-Gren and the Fyssen Foundations, the Department of Mineral Resources (Bangkok) and TRF-CNRS Project.

Competing interests statement The authors declare that they have no competing financial interests.

Correspondence and requests for materials should be addressed to J.-J.J. (e-mail: jaeger@isem.univ-montp2.fr).

Species interactions can explain Taylor's power law for ecological time series

A. M. Kilpatrick & A. R. Ives

Department of Zoology, University of Wisconsin—Madison, Madison, Wisconsin 53706, USA

One of the few generalities in ecology, Taylor's power law[1–3], describes the species-specific relationship between the temporal or spatial variance of populations and their mean abundances. For populations experiencing constant per capita environmental variability, the regression of log variance versus log mean abundance gives a line with a slope of 2. Despite this expectation, most species have slopes of less than 2 (refs 2–4), indicating that more abundant populations of a species are relatively less variable than expected on the basis of simple statistical grounds. What causes abundant populations to be less variable has received considerable attention[5–12], but an explanation for the generality of this pattern is still lacking. Here we suggest a novel explanation for the scaling of temporal variability in population abundances. Using stochastic simulation and analytical models, we demonstrate how negative interactions among species in a community can produce slopes of Taylor's power law of less than 2, like those observed in real data sets. This result provides an example in which the population dynamics of single species can be understood only in the context of interactions within an ecological community.

Taylor's power law describes the species-specific scaling relationship between the variance of population abundances and their means, which has been established for more than 400 species in taxa ranging from protists to vertebrates[2,3]. The ubiquity of Taylor's power-law slopes of between 1 and 2 suggests an underlying fundamental explanation that might give insights into general ecological processes affecting many species. Furthermore, understanding the relationship between a population's variability and its mean abundance is needed to address numerous ecological problems, including conducting population viability analyses in conservation biology[13], testing diversity–stability hypotheses[14–16] and sampling for pests in agriculture[17,18].

There are two separate relationships between the variance and mean of a species's abundance, one temporal and one spatial[3]. Of these, the spatial relationship has received the most theoretical investigation[5,7–12,19]. Here we focus on the temporal relationship in which the variance and mean abundance of a species through time are calculated for multiple populations, and these are graphed on a log–log scale with each datum representing a population. The null expectation for Taylor's power law for temporal variation is that the slope of the log variance versus log mean plot equals 2. This expectation derives from the well-known relationship that, when scaling any random variable X with finite mean μ and variance σ^2 by some constant k, the mean and variance of kX are $k\mu$ and $k^2\sigma^2$, respectively. On a log–log plot, the relationship between $k\mu$ and $k^2\sigma^2$ is a line with a slope of 2. A slope of less than 2 indicates that the per capita variability in population abundance decreases with increasing mean population abundance.

Taylor and others[3,4] showed that the logarithm of the temporal variance of a population is tightly correlated to the logarithm of the mean abundance, with the correlation coefficient usually exceeding 0.9. For most species, the slope of the relationship is between 1 and 2. In an attempt to explain slopes of less than 2, Anderson and coworkers[12] showed that demographic stochasticity (variation caused by stochastic births and deaths of individuals in finite populations) in an exponentially growing population could lead to slopes for the temporal log variance versus log mean relationship of between 1 and 2, depending on the size of the population and the demographic parameters. Although demographic stochasticity certainly affects the dynamics of populations and can produce reduced slopes of Taylor's power law[12,20,21], these effects are most prevalent for population sizes on the order of hundreds or smaller. For many of the species considered by Taylor and others[3,4], the population size being sampled is likely to be in the tens of thousands or greater (for example, many insect species). For larger population sizes, environmental stochasticity in per capita population growth rates, which leads to a variance that scales with the square of the mean, overshadows the variance due to demographic stochasticity, which scales directly with the mean.

A second mechanism that could decrease the slope of Taylor's power law is sampling variance or error in the measurement of population abundance[22]. Sampling variance generally scales directly with the mean and thus by itself would produce a power-law slope of less than 2. Nevertheless, the effect of sampling variance on the slope declines with sampled abundance because at high abundance the variance–mean scaling will be dominated by environmental and/or demographic stochasticity. Although sampling variance certainly

contributes to the relationships seen in the empirical data, it is unlikely to be important in data sets where the sampled abundance is high.

Here we demonstrate that negative species interactions, including direct competition and 'apparent competition' through shared predators, lead to slopes of the log variance versus log mean relationship of between 1 and 2. Negative species interactions are common in natural communities[23], and thus this mechanism might affect the variance–mean scaling of many species. For example, power-law slopes of less than 2 have been demonstrated for numerous aphids in Europe[3,4], and many aphids are known to compete both directly[24] and indirectly[25]. Certainly, for some species, a power-law slope of less than 2 is unlikely to be caused by negative species interactions, but many other species have direct competitors and shared predators that could affect their power-law slopes.

For the simplest case, we considered a competitive community of n species each growing according to a discrete logistic equation in which carrying capacities K_i differ between species. The density of species i at time $t+1$, $x_i(t+1)$, is given by

$$x_i(t+1) = x_i(t)\exp\left[r_i\left(1 - \frac{x_i(t) + \sum_{j\neq i}\alpha_{ij}x_j(t)}{K_i}\right) + \varepsilon_i(t)\right] \quad (1)$$

where r_i is the intrinsic rate of increase of species i, α_{ij} is the competition coefficient giving the per capita effect of species j on species i (which possibly differs between each pair of species) and $\varepsilon_i(t)$ is a normal random variable incorporating environmental stochasticity into the per capita population growth rate.

To simulate the data needed to calculate the temporal Taylor's power law, we embedded a focal species in different simulated communities. The focal species retained its intrinsic rate of increase, r_i, in each of these communities, but values of K_i and α_{ij} for the focal and all other species were selected from random distributions. One example of the resulting simulations (Fig. 1) with average $\alpha_{ij} = 0.25$ creates data corresponding to Taylor's power law with a slope of 1.58. Note that even though interspecific competition created a slope of less than 2, the strength of competition is weak (average $\alpha_{ij} = 0.25$). Furthermore, the average correlation coefficient between the focal species and all other species in the community (averaged over all five communities) is +0.04, giving no visual suggestion of a strong effect of competition on the temporal dynamics of the species.

Our simulations produce linear relationships between log variance and log mean comparable to those observed for a number of real species (Fig. 2a,b). When there are no species interactions (that is, $\alpha_{ij} = 0$), the slope of the temporal relationship between log variance and log mean averages 2 (Fig. 2c) but might be above or below 2 for a single set of simulations. However, when competitive interactions increase between species, the average slope decreases from 2 to 1 (Fig. 2c). Real single-species data sets show a range of slopes from 0.9 to 2.6, with most between 1.0 and 1.8 (ref. 3). Thus, the range of values described for real species could be the result of species existing in communities with strong to weak competition.

To explore the general relationships underlying these simulation

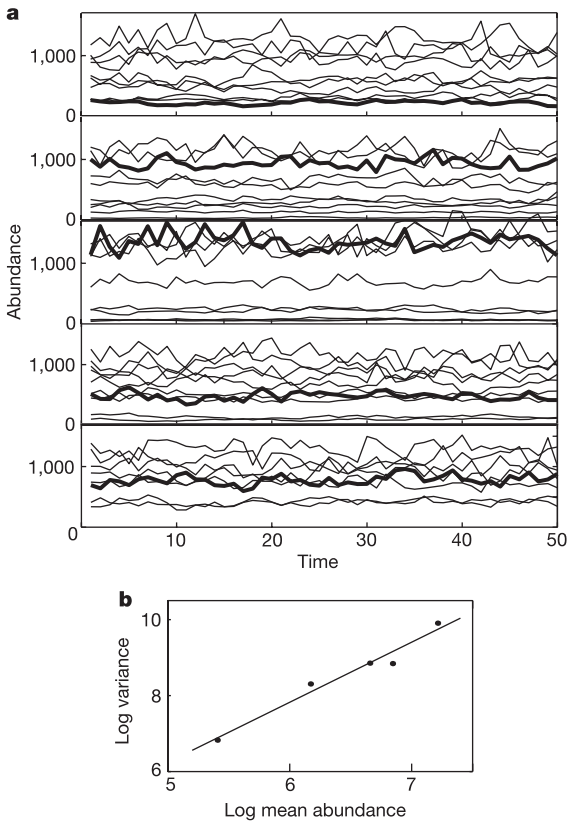

Figure 1 Five simulations of ten-species communities using the model from equation (1). **a**, Each species in the collection of simulations had a fixed r_i between 0.5 and 1.0 for all five simulations. In each simulation, corresponding to separate communities, the values of α_{ij} and K_i were selected from uniform distributions with ranges of 0–0.5 and 50–1,550, respectively. For the focal species, plotted with the thick solid line in each panel, $r = 0.57$ in all five communities. **b**, Plot of log variance against log mean for this species, with each point giving the log mean and log variance from one of the five other panels. The slope of the best-fit line is 1.58.

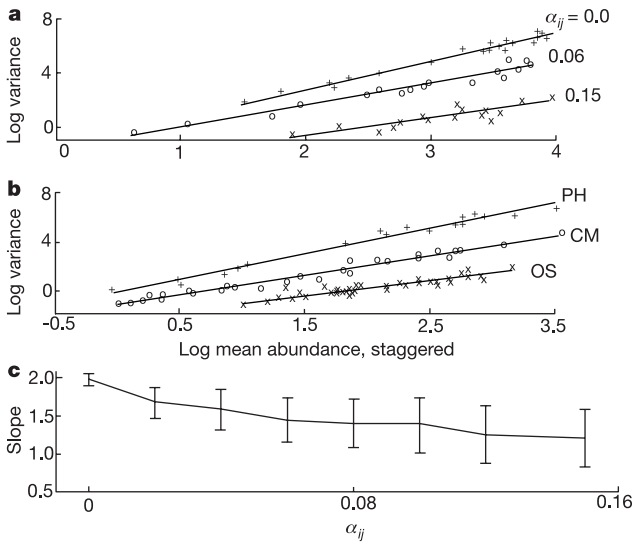

Figure 2 Taylor's power law for real and simulated data. **a**, **b**, Log temporal variance plotted against log mean abundance for simulations using equation (1) (**a**) and empirical data from three representative insect species from ref. 13 (**b**). PH, *Phorodon humuli*; CM, *Colostygia multistrigaria*; OS, *Ourapteryx sambucaria*. The mean abundances have been staggered horizontally for clarity. Parameter values from equation (1) were set to match the range in mean and variance for the data presented in **b**: plus signs, $\varepsilon \sim N(0, 0.006)$, $K \sim$ uniform (50–5,050); $\alpha_{ij} = 0$; circles, $\varepsilon \sim N(0, 0.006)$, $K \sim$ uniform (50–2,050), $\alpha_{ij} = 0.06$; crosses, $\varepsilon \sim N(0, 0.004)$, $K \sim$ uniform (50–1,050), $\alpha_{ij} = 0.15$. **c**, The slope (±1 s.d.) of the plot of log temporal variance versus log mean abundance as a function of the average strength of competition between species, with $K \sim$ uniform (50–1,050). All simulations were done starting with 20 species, and temporal variance and mean were calculated from 50 time steps for each population after transients had dissipated.

results, we developed a log–linear approximation model that can be solved algebraically (see Methods). The solution incorporates the average strength of interspecific competition as the reduction in the average of the equilibrium densities of species in the community scaled by their carrying capacities. Thus, denoting $\bar{x}^* = \frac{1}{n}\sum_{i=1}^{n} \frac{x_i^*}{K_i}$, where x_i^* is the equilibrium abundance of species i (that is, the abundance that would occur in the absence of environmental variability), if there is no interspecific competition then $\bar{x}^* = 1$, and the greater the strength of interspecific competition averaged throughout the community, the lower is the value of $\bar{x}^*$. The analysis shows that the power-law slope decreases with increasing strength of interspecific competition, as measured by the reduction in $\bar{x}^*$, yet it is relatively insensitive to the number of species in a community once the community size, n, exceeds five (Fig. 3a). The extent to which competition decreases the slope also depends on how the stochastic variation affecting species densities is correlated: when the environmental stochasticity is perfectly correlated between species ($\rho = 1$), the slope equals 2, and decreasing environmental correlation decreases the slope (Fig. 3b). This shows, interestingly, that the slope of the relationship between log variance and log mean might be the product not only of species interactions but also of how species respond to environmental stochasticity relative to each other. Finally, higher intrinsic rates of increase lessen the effect of competition in decreasing the slope below 2 (Fig. 3b). These results hold for a broad suite of possible models of competitive interactions (see Methods). Furthermore, simulations of communities in which species do not interact directly but instead interact through shared predators show that indirect 'apparent competition' can produce power-law slopes of less than 2 in much the same way as direct competition does (results not shown).

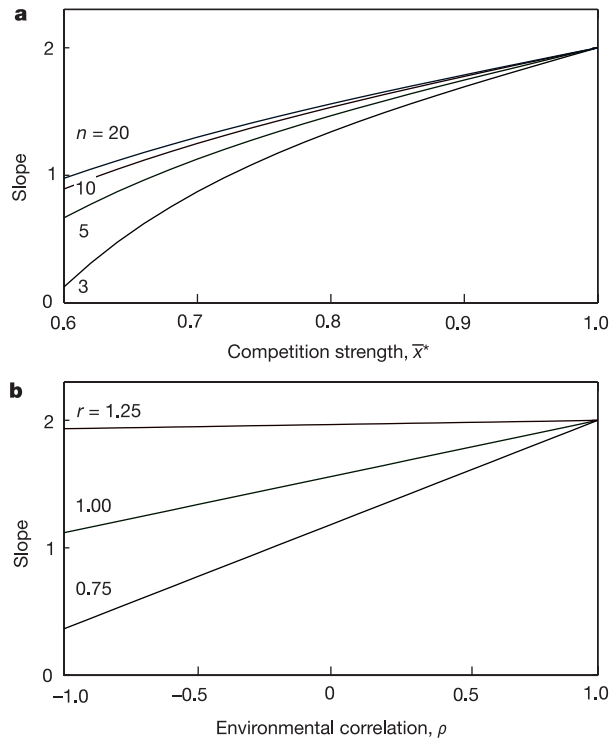

Figure 3 Analytical approximation of Taylor's power law (equations (5) and (6)). **a**, Slope of Taylor's power law plotted against the strength of competition measured by the decrease in mean species densities relative to their carrying capacities, $\bar{x}^*$, for communities with $n = 3$, 5, 10 and 20 species. Other parameters are $r = 1$ and $\rho = 0$. **b**, Slope of Taylor's power law plotted against the correlation between environmentally driven variation in species per capita population growth rates, ρ, for $r = 1.25$, 1.00 and 0.75. Other parameters are $n = 20$ and $\bar{x}^* = 0.8$.

The effect of competitive interactions on the slope of Taylor's power law can be explained by considering the simple case of a community consisting of only two competitors. Suppose one competitor is less abundant, either because it has a smaller carrying capacity K_i or because it is an inferior competitor to the other species owing to asymmetric values of α_{ij}. The variability experienced by the rarer species is a combination of the environmental variability that affects it directly and the variability produced by competition with the more common species. Because the more common species has a higher carrying capacity and/or is a superior competitor, the variability in the rare species produced by interspecific competition is relatively large, and this substantially increases the variance in abundance of the rarer species. In contrast, the more common species experiences weaker interspecific competition and therefore has lower variability. Thus, the higher variability that the rarer species experiences through interspecific competition relative to the more common species produces a Taylor's power-law slope of less than 2. Although this example consists of two species in one community, the same reasoning applies to one species existing in two communities at different abundances.

In conclusion, our result contributes to the growing understanding that weak or diffuse interactions between species in a food web can contribute strongly to the dynamical properties of a community as a whole or its constituent species[26–28]. If interspecific competition influences the slope of Taylor's power law for a given species, this species-specific slope is in fact governed by multi-species interactions. This raises caution about performing analyses involving the stochastic fluctuations in species population densities, such as population viability analyses[13], because a species's stochastic dynamics might reflect not only the species's sensitivity to its environment but also its interactions with other species. Thus, to understand fluctuations in the abundance of individual species, it is necessary to understand how species interact with each other and how environmental variability is propagated through food webs. □

Methods

To analyse the competition model in equation (1), we first note that, without loss of generality, population densities, $x_i(t)$, can be rescaled relative to their carrying capacities, K_i, to give $\hat{x}_i(t) = x_i(t)/K_i$. Rescaling $\hat{\alpha}_{ij} = \alpha_{ij}K_j/K_i$ gives an equation of the form of equation (1) but without parameters K_i. The rescaled coefficients $\hat{\alpha}_{ij}$ give the competitive effect of species j on species i weighted by the relative densities that each species would achieve in the absence of competition. Therefore, $\hat{\alpha}_{ij}$ measures the impact of interspecific competition relative to intraspecific competition.

Nearly all nonlinear models can be well approximated by Taylor expanding around a fixed point. For a model of n interacting species such as equation (1), the population dynamics can be approximated by the log–linear model

$$z_i(t+1) = \sum_{j=1}^{n} b_{ij} z_j(t) + \varepsilon_i(t) \tag{2}$$

where $z_i(t) = \log \hat{x}_i(t)$, $\varepsilon_i(t)$ is a random variable representing environmental stochasticity, and b_{ij} encapsulates the interactive effect of species j on the population growth rate of species i.

For the specific model in equation (1), we consider the special case in which $r_i = r$ and $\hat{\alpha}_{ij} = \hat{\alpha}_j$ for all species i. That is, all species have the same intrinsic rate of increase, and the relative competitive effect of species j on species i is the same for all species i. We consider this special case because it leads to an algebraic solution of equation (2). Numerical studies of the general form of equation (1) demonstrate the same qualitative patterns as derived from this special case. When $r_i = r$ and $\hat{\alpha}_{ij} = \hat{\alpha}_j$, coefficients in the log–linear approximation are

$$\left.\begin{aligned} b_{ij} &= 1 - r\hat{x}_i^* \quad (i = j) \\ b_{ij} = b_j &= -r\left(\tfrac{1-n\bar{x}^*}{n-1} + \hat{x}_j^*\right) \quad (i \neq j) \end{aligned}\right\} \tag{3}$$

where $\hat{x}_i^*$ is the untransformed equilibrium abundance of species i (scaled by K_i) in the absence of environmental stochasticity, and $\bar{x}^*$ is the mean of the values of $\hat{x}_i^*$ across all species. This approximation has the properties that $b_{ij} = b_j$ and $b_{ii} + \sum_{j\neq i} b_{ij} = 1 - r$, which are properties shared by all competition models of the form

$$\hat{x}_i(t+1) = \hat{x}_i(t) f\left[\hat{x}_i(t) + \sum_{j\neq i} \hat{\alpha}_j \hat{x}_j(t)\right] \tag{4}$$

where $f[\,]$ is an unspecified linear or nonlinear function.

The change in the variance relative to the change in the mean can be computed from equations (2) and (3) as

$$\frac{\Delta V[z_i]}{\Delta \bar{z}_i} = \frac{(2n(n+1)-6n+2)(\rho-1)(r(\bar{x}^* n-1)-(n-1))}{r(\bar{x}^* n-1)((n-2)+\bar{x}^* n-r(\bar{x}^* n-1))(r(\bar{x}^* n-1)-2(n-1))} \quad (5)$$

where $\Delta V[z_i]$ is the change in the variance of the log-transformed population density $z_i(t)$ with a change $\Delta \bar{z}_i$ in the mean, and ρ is the correlation of environmental stochasticity $\varepsilon_i(t)$ between species (assumed to be the same for all species in the community). This is an exact solution for the model given in equations (2) and (3) that can be derived algebraically for the cases of $n = 2$ and $n = 3$ (ref. 29), and then generalized to arbitrarily many species. The slope of the variance versus the mean population density on a logarithmic scale is

$$\frac{\Delta \log V[x_i]}{\Delta \log \bar{x}_i} \cong 2 + \frac{\Delta V[z_i]}{\Delta \bar{z}_i} \quad (6)$$

allowing the translation of equation (5) into Taylor's power law.

Received 20 September 2002; accepted 28 January 2003; doi:10.1038/nature01471.

1. Taylor, L. R. Aggregation, variance and the mean. *Nature* **189,** 732–735 (1961).
2. Taylor, L. R., Woiwod, I. P. & Perry, J. N. The density-dependence of spatial behaviour and the rarity of randomness. *J. Anim. Ecol.* **47,** 383–406 (1978).
3. Taylor, L. R. & Woiwod, I. P. Comparative synoptic dynamics: 1. Relationships between interspecific and intraspecific spatial and temporal variance-mean population parameters. *J. Anim. Ecol.* **51,** 879–906 (1982).
4. Taylor, L. R. & Woiwod, I. P. Temporal stability as a density-dependent species characteristic. *J. Anim. Ecol.* **49,** 209–224 (1980).
5. Gillis, D. M., Kramer, D. L. & Bell, G. Taylor's Power Law as a consequence of Fretwell's ideal free distribution. *J. Theor. Biol.* **123,** 281–288 (1986).
6. Perry, J. N. Some models for spatial variability of animal species. *Oikos* **51,** 124–130 (1988).
7. Taylor, R. A. J. The behavioural basis of redistribution: 1. The DELTA-model concept. *J. Anim. Ecol.* **50,** 573–586 (1981).
8. Taylor, R. A. J. The behavioural basis of redistribution: 2. Simulations of the DELTA-model. *J. Anim. Ecol.* **50,** 587–604 (1981).
9. Perry, J. N. Chaotic dynamics can generate Taylor's power law. *Proc. R. Soc. Lond. B* **257,** 221–226 (1994).
10. Taylor, L. R. & Taylor, R. A. J. Aggregation, migration and population mechanics. *Nature* **265,** 415–421 (1977).
11. Hanski, I. Spatial patterns and movements in coprophageous beetles. *Oikos* **34,** 293–310 (1980).
12. Anderson, R. M., Gordon, D. M., Crawley, M. J. & Hassell, M. P. Variability and the abundance of animal and plant species. *Nature* **296,** 245–248 (1982).
13. Beissinger, S. R. & McCullough, D. R. (eds) *Population Viability Analysis* (Univ. Chicago Press, Chicago, 2002).
14. Ives, A. R. & Hughes, J. B. General relationships between species diversity and stability in competitive systems. *Am. Nat.* **159,** 388–395 (2002).
15. McCann, K. S. The diversity-stability debate. *Nature* **405,** 228–233 (2000).
16. Tilman, D. Biodiversity: Population versus ecosystem stability. *Ecology* **77,** 350–363 (1996).
17. Taylor, L. R. Synoptic dynamics, migration and the Rothamsted insect survey. *J. Anim. Ecol.* **55,** 1–38 (1986).
18. Green, R. H. Power analysis and practical strategies for environmental monitoring. *Environ. Res.* **50,** 195–206 (1989).
19. Thorarinsson, K. Population density and movement: A critique of DELTA-models. *Oikos* **46,** 70–81 (1986).
20. Keeling, M. & Grenfell, B. Stochastic dynamics and a power law for measles variability. *Phil. Trans. R. Soc. Lond. B* **354,** 769–776 (1999).
21. Keeling, M. J. Simple stochastic models and their power-law type behaviour. *Theor. Popul. Biol.* **58,** 21–31 (2000).
22. Titmus, G. Are animal populations really aggregated? *Oikos* **40,** 64–68 (1983).
23. Schoener, T. W. Field experiments on interspecific competition. *Am. Nat.* **122,** 240–285 (1983).
24. Gianoli, E. Competition in cereal aphids (Homoptera: Aphididae) on wheat plants. *Environ. Entomol.* **29,** 213–219 (2000).
25. Muller, C. B. & Godfray, H. C. J. Apparent competition between two aphid species. *J. Anim. Ecol.* **66,** 57–64 (1997).
26. McCann, K., Hastings, A. & Huxel, G. R. Weak trophic interactions and the balance of nature. *Nature* **395,** 794–798 (1998).
27. Berlow, E. L. Strong effects of weak interactions in ecological communities. *Nature* **398,** 330–334 (1999).
28. Ives, A. R., Gross, K. & Klug, J. L. Stability and variability in competitive communities. *Science* **286,** 542–544 (1999).
29. Ives, A. R., Dennis, B., Cottingham, K. L. & Carpenter, S. R. Estimating community stability and ecological interactions from time-series data. *Ecol. Monogr.* (in the press).

Acknowledgements This manuscript was improved by the comments of B. Cardinale, K. Gross, L. Angeloni, A. Forbes and C. Williams. Funding was provided by the US National Science Foundation.

Competing interests statement The authors declare that they have no competing financial interests.

Correspondence and requests for materials should be addressed to A.M.K. (e-mail: amkilpatrick@wisc.edu) or A.R.I. (e-mail: arives@wisc.edu).

Engineering evolution to study speciation in yeasts

Daniela Delneri*†, Isabelle Colson*†‡, Sofia Grammenoudi*‡, Ian N. Roberts§, Edward J. Louis‖ & Stephen G. Oliver*

** School of Biological Sciences, University of Manchester, 2.205 Stopford Building, Oxford Road, Manchester M13 9PT, UK*
§ National Collection of Yeast Cultures, Institute of Food Research, Norwich Research Park, Colney, Norwich NR4 7UA, UK
‖ Department of Genetics, University of Leicester, University Road, Leicester LE1 7RH, UK
† These authors contributed equally to this work

The *Saccharomyces* '*sensu stricto*' yeasts are a group of species that will mate with one another, but interspecific pairings produce sterile hybrids. A retrospective analysis of their genomes revealed that translocations between the chromosomes of these species do not correlate with the group's sequence-based phylogeny[1] (that is, translocations do not drive the process of speciation). However, that analysis was unable to infer what contribution such rearrangements make to reproductive isolation between these organisms. Here, we report experiments that take an interventionist, rather than a retrospective approach to studying speciation, by reconfiguring the *Saccharomyces cerevisiae* genome so that it is collinear with that of *Saccharomyces mikatae*. We demonstrate that this imposed genomic collinearity allows the generation of interspecific hybrids that produce a large proportion of spores that are viable, but extensively aneuploid. We obtained similar results in crosses between wild-type *S. cerevisiae* and the naturally collinear species *Saccharomyces paradoxus*, but not with non-collinear crosses. This controlled comparison of the effect of chromosomal translocation on species barriers suggests a mechanism for the generation of redundancy in the *S. cerevisiae* genome[2].

The *Saccharomyces sensu stricto* yeasts comprise six species: *S. cerevisiae*, *S. paradoxus*, *S. bayanus*, *S. cariocanus*, *S. mikatae* and *S. kudriavzevii*[3,4]. Three of these species are characterized by the presence of specific reciprocal chromosomal translocations: four in *S. bayanus* and *S. cariocanus*, and one and two, respectively, for the two strains of *S. mikatae*—IFO1815 and IFO1816 (ref. 1). Reciprocal translocations in yeasts can potentially have a significant effect on reproductive isolation, and have been proposed as a cause of speciation, by inducing inviability of hybrid ascospores[5]. Yeasts from the *Saccharomyces sensu stricto* species readily hybridize in nature and in the laboratory, but hybrids are generally sterile, with less than 5% viable ascospores[6–8]. We previously mapped the translocations, relative to the karyotype of *S. cerevisiae*, which are found in the *Saccharomyces sensu stricto* yeasts[1], and discovered that there was no correlation between the sequence-based phylogeny of these species and the occurrence of chromosomal translocations. We concluded that chromosomal translocations do not drive the process of speciation, but may contribute to the reproductive isolation between species once they had formed by some other means. To analyse that contribution, we required some way of dissecting the effects of reciprocal translocations away from the other genetic differences between these species. Fortunately, the availability of the complete genome sequence of *S. cerevisiae*[2], and our own development of a method for generating precisely located chromosomal translocations in this organism[9], offered the opportunity for effecting such a dissection. We could engineer the genome of *S. cerevisiae* to make it collinear with that of one of the other

‡ Present addresses: School of Biological Sciences, University of Wales at Bangor, Brambell Building, Deiniol Road, Bangor LL57 2UW, UK (I.C.); Alexander Fleming Biomedical Science Research Centre, 14–16 Fleming Street, 16672-Vari, Greece (S.G.).